Journal of Computational Methods in Sciences and Engineering 7 (2007) 443–462
IOS Press

Orbital degeneracy and magnetic properties of potassium clusters incorporated into nanoporous crystals of zeolite A

Takehito Nakano* and Yasuo Nozue
Department of Physics, Graduate School of Science, Osaka University, Toyonaka, Osaka 560-0043, Japan

Received 29 June 2007
Revised /Accepted 6 September 2007

Abstract. Potassium nanoclusters in aluminosilicate zeolite A shows ferromagnetic properties, although bulk metal of K is nonmagnetic. K clusters are prepared by adsorbing guest K atoms into the supercages (α cages) of dehydrated zeolite A, where supercages with the inside diameter of $\sim$ 11 Å are arrayed in a simple cubic structure. By the loading of guest K atoms, s-electrons are provided for clusters, and successively occupy $1s$- and $1p$-like quantum states of cluster. The average number of guest K atoms in a cluster, n, is widely controlled up to 7.2. This material shows ferromagnetism at $n > 2$ at low temperatures, where s-electrons in the $1p$ state of clusters are responsible for the ferromagnetism. We have found a fine step at $n = 2$ in magnetization and g value. The g values of ferromagnetic samples with $2 < n < 6$ obviously decrease from 2 at low temperatures, indicating that an enhancement of the spin-orbit interaction (SOI) occurs due to the orbital degeneracy of the $1p$ state. An enhancement mechanism is proposed based on the Schmidt orthogonalized wave function. In the ferromagnetic sample, an anomalously large magnetization is observed at higher magnetic fields up to 52 T at low temperatures. The level crossing of *LS* multiplet terms in the degenerate $1p$ orbital of cluster is proposed as the possible origin of the anomalous increase in magnetization at higher fields. The ferromagnetism coexists with antiferromagnetic coupling between magnetic moments of clusters. The origin of the spontaneous magnetization of the ferromagnetism is interpreted in terms of spin-canting mechanism where the Dzyaloshinsky-Moriya interaction is strongly enhanced by the degenerate $1p$ orbital of K cluster. Possible structures of K cluster in the supercage are also discussed for the orbital degeneracy of $1p$ state.

Keywords: Alkali-metal cluster, zeolite, electronic property, quantum size effect, orbital degeneracy, ferromagnetism, ferrimagnetism, Mott-Hubbard insulator

1. Introduction

Novel electronic properties of alkali metal clusters stabilized in the nanospaces of zeolite crystals have attracted a deep interest. Generally, in alkali- and noble-metal clusters, the quantum size effect leads to discrete energies of conduction electrons, and there appear new properties characteristic of electronic shell structures [1–3]. Electronic properties of these clusters are quite different from those of the atoms as well as those of bulk metals. The electronic shell structure of alkali-metal cluster has been well calculated by the jellium background model [3,4], where positive charges of cations are replaced by a

*Corresponding author. Tel.: +81 6 6850 5534; Fax: +81 6 6850 5376; E-mail: nakano@nano.phys.sci.osaka-u.ac.jp.

uniformly distributed positive background with the size of cluster. The quantum electronic states $1s$, $1p$, $1d$, $2s$, $1f$ etc. appear in the increasing order of energy in the spherical jellium background model [3,4], where p, d and f states exhibit an appearance of orbital angular momentum of confined s-electrons. The jellium model gives us quite simple and clear insight, but some of electronic properties are sometimes out of insight, because of the fine atomic structure of actual clusters.

In the free cluster experiments, a mass spectroscopy has a great advantage in their size selectivity. The photoionization, photodissociation and photoelectron spectroscopies of free clusters have a great contribution to clarify the electronic shell structures of alkali-metal clusters [1,5]. Usually, such experiments are not applicable to the studies of clusters embedded in matrices. Matrix-supported metal clusters, however, can provide us a wide variety of direct physical measurements with varying temperature, such as optical, magnetic, electron spin resonance experiments.

The quantum size effect in metal clusters is essentially important for the understanding of magnetic properties [6,7]. The clusters of non-magnetic elements can exhibit magnetic moments when they have an odd number of electrons, for example, and are expected to show quite different temperature dependence of magnetic susceptibility compared to that in bulk metal [6]. Several kinds of materials have been used as the matrixes of alkali-metal clusters. One of the typical and clean matrixes is rare gases, where the clusters are formed by the simultaneous condensation with alkali-metal vapor on to a low temperature substrate. The detailed studies on optical [8] as well as electron spin resonance [9] were carried out on these matrix-isolated alkali-metal clusters to investigate the quantum electronic states, the surface plasmon excitations, g values, hyperfine coupling, geometry of the cluster and their size-dependence and so on. Ordinary matrix-supported alkali-metal clusters, however, have a wide size distribution which obscures their properties.

Alkali-metal clusters stabilized in the nanoporous crystals of aluminosilicate zeolites have a great advantage. Zeolite is crystalline and has regularly arrayed nanospaces with the well-defined size. Mutual interaction between arrayed clusters can lead to macroscopic phenomena, such as magnetic ordering and metal-insulator transition. We can control average number of atoms involved in clusters by adjusting the loading density. We can choose different sizes and different types of array of nanospace by selecting zeolites, such as zeolite A with a simple cubic array of cages having 11 Å inner size, zeolite X with a diamond structure array of cages having 13 Å inner size, etc. In the present paper, we concentrate on the electronic properties of K clusters incorporated into zeolite A (structural type code LTA). This material is known to show ferromagnetism [10]. Recent studies have revealed that the orbital degeneracy of the $1p$-like state of K cluster plays an essential role in the appearance of the ferromagnetism.

The present paper is organized as follows. In Section 2, we explain the feature of zeolite crystals as the host material of alkali-metal clusters. The optical properties and the basic electronic states of K clusters in zeolite A are briefly summarized in Section 3. In Section 4, we discuss the spin-orbit interaction (SOI) and the orbital degeneracy of the $1p$-like state of K clusters from the results of electron spin resonance. The enhancement mechanism of SOI is discussed in Section 5. The SOI and the orbital degeneracy provide an anomalous magnetization at the high-magnetic field up to 52 T in Section 6. The origin of the ferromagnetism of K clusters in zeolite A is discussed in Section 7 by taking account of the orbital degeneracy of the $1p$-like state. Magnetically ordered states found in alkali-metal clusters in other zeolites are also briefly mentioned at the end of Section 7, and some comments are given from the viewpoint of degenerate orbital of cluster. A summary is given in Section 8.

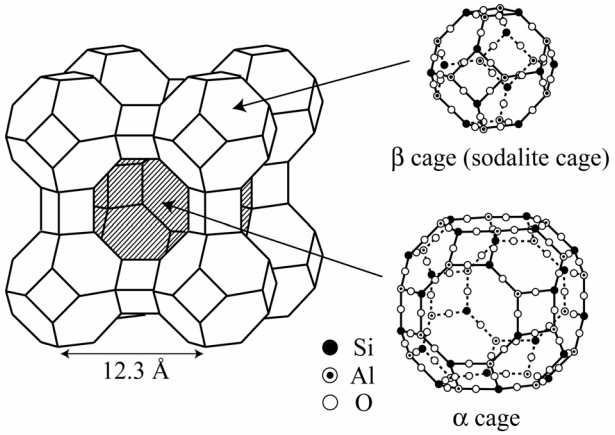

Fig. 1. Schematic illustration of the framework structure of aluminosilicate zeolite A. The framework has the LTA-type structure. Closed circles, open circles and those with dots show Si, O and Al atoms, respectively. Alkali cations are not shown here. The cation sites are explained in Fig. 4 in detail.

2. Zeolite crystals as the matrix of alkali metal clusters

Most of zeolite crystals are aluminosilicates, where the well-defined cages or channels with the size of nanometer are regularly arrayed. Many types of zeolite crystals are synthesized under various growth conditions. They are widely used as molecular sieves, catalysts, adsorbents, builders of detergents and so on [11]. A general chemical formula of aluminosilicate zeolites is given by $A_a\mathrm{Al}_a\mathrm{Si}_b\mathrm{O}_{2(a+b)}$, where A stands for exchangeable alkali cations, such as Na^+ or K^+. Cations are distributed in the space of the negatively charged framework $\mathrm{Al}_a\mathrm{Si}_b\mathrm{O}_{2(a+b)}$ for the charge compensation. Figure 1 shows a schematic illustration of the framework structure of zeolite A (structural type code LTA). Chemical formula of the primitive unit of structure (β cage) is given by $a = b = 12$. Closed circles, open circles and those with dots show Si, O and Al atoms, respectively. In the LTA-type structure, β cages with the inside diameter of ~ 7 Å are connected through the double 4-membered ring with each other, and arrayed in a simple cubic structure. Then, the α cages (supercages) with the inside diameter of ~ 11 Å are formed among the β cages. The α cages are connected by the sharing of the 8-membered ring with each other, and arrayed also in a simple cubic structure. The lattice constant is 12.3 Å. K clusters in zeolite A are generated by the loading of K atoms into completely dehydrated K-type zeolite A (K-form A) at the number density of n per α cage. The final chemical formula is given by $\mathrm{K}_{12+n}\mathrm{Al}_{12}\mathrm{Si}_{12}\mathrm{O}_{48}$. The number density of α cage (or β cage) is $5.4 \times 10^{20}\mathrm{cm}^{-3}$. The cations are not shown in Fig. 1, but the structure of zeolite cations and loaded guest atoms play an important role in the degeneracy of $1p$-like state of s-electron as well as the confinement potential for s-electrons, as explained in Section 4 in detail.

By adsorbing the guest alkali atoms into zeolite crystals, the s-electrons are shared among many cations and confined in the cages. Cationic alkali-metal nanoclusters are generated in the cages of zeolite. Optical and magnetic properties have been investigated for various alkali metal clusters in zeolites [10,12–24]. Zeolites are thought to be one of the most ideal host matrices or containers of alkali metal nanoclusters. The advantages of the use of zeolite matrices are listed as follows. (1) The maximum size of the cluster is restricted by the size of the zeolite cage, which leads to the equivalent size distribution of clusters. (2) The average number of s-electrons per cluster can be controlled at a rather wide range, up to around 10, by controlling the loading density of guest alkali metal. (3) The clusters can be generated at very high number-density, $\sim 10^{21}\mathrm{cm}^{-3}$, which gives an enough signal-intensity for various kinds of physical

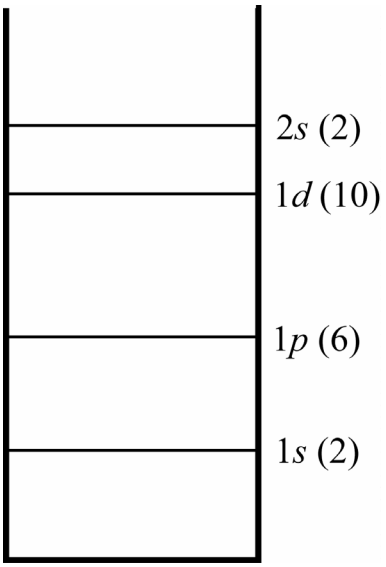

Fig. 2. One-electron quantum states of spherical well potential with the infinite depth. The states $1s$, $1p$, $1d$ etc. appear in the increasing order of energy. The degeneracy including the spin is shown in the parentheses.

measurements. (4) The clusters can be periodically arrayed, called a 'cluster crystal' [25], and they have a mutual interaction through the windows of the cages. Totally, clusters in zeolites can result in macroscopic phenomena such as metallic phase transition and magnetic orderings [10,20,26,27]. A microscopic insight of alkali metal clusters is very important to understand such macroscopic properties. Macroscopic properties are quite unique ones in the solid state physics.

3. Optical properties and electronic states of potassium clusters in zeolite A

When guest K atoms are adsorbed into K-form zeolite A, $4s$ electrons of the K atoms are shared among several K^+ cations in α cage and repulsed by the negatively charged framework. A cationic K cluster is generated in the α cage. The value of n is equal to the average number of s-electrons per cluster. The primitive electronic states of K cluster in zeolite A can be well explained by assuming that electrons are confined in the spherical-well potential with the inside diameter of α cage, 11 Å. This resembles the jellium-background model, but the potential well is formed not only by the attractive force of alkali cations but also by the repulsive force of negatively charged zeolite framework which gives the wall of the potential well. The quantum states $1s$, $1p$, $1d$ and so on appear in the increasing order of energy as shown in Fig. 2. The states $1s$, $1p$ and $1d$ have the degeneracy of 2, 6 and 10, respectively, including spin as shown in the parentheses in Fig. 2. When we set the inside diameter of the spherical well potential as 11 Å, which is same as that of the α cage, the energy difference between $1s$ and $1p$ states is calculated to be 1.2 eV.

Optical properties of K clusters in zeolite A have been investigated in detail with changing systematically the K-loading density [28]. A significant absorption band is observed at infrared region 1.2 eV in dilutely K-loaded K-form zeolite A. There was no absorption at visible and ultra-violet regions. This absorption band can be explained by neither K atom nor bulk K metal. This band is assigned to the $1s$-to-$1p$ allowed transition of K clusters formed in the α cage. The value of n can be controlled up

to $\sim$ 7.2 in K-form zeolite A. With increasing K-loading density, new bands at 1.5 and 2.0 eV grown systematically with n are observed at $n > 2$ in the optical reflection spectra [28]. They are assigned to the $1p$-$1d$ transition of K cluster. The band at 2.0 eV has large oscillator strength, and is explained by the surface plasmon-like excitation which is the collective motion of electrons confined in cluster. These results clearly show the successive occupation of $1s$ and $1p$ states by s-electrons with increasing n, where the first two electrons occupy the $1s$ state and the next electrons the $1p$ state. This is the shell model. A finite contribution of the Drude term is extracted from the analysis of reflection spectrum down to 0.5 eV [28]. However, there is no direct evidence of the Drude-like metallic absorption. The Urbach tail absorption was observed down to 0.3 eV at any values of n [29,30], indicating the Mott-Hubbard type insulator of magnetic materials. Even at much lower energies, a metallic absorption was not observed down to 0.05 eV in K clusters, but a metallic absorption has been observed in Rb and Cs clusters [24].

Adjacent α cages are connected at the window of 8-membered ring. This may lead to the mutual overlapping of cluster wave functions. A finite energy band width of electrons localized in K clusters can be expected, according to the analogy of tight-binding model. Recently, Arita et al. [31] have performed the first-principles band calculation on non-loaded and K-loaded zeolite A. The calculated band structures are surprisingly simple and consistent with the tight-binding model formed by the $1s$ and $1p$ electronic states of clusters. They expressed this result as "supercrystal", namely the crystal of "superatoms". If the value of n is equal to 2, $1s$ state is fully occupied as the closed shell cluster. The sample is expected to be an ordinary band insulator. When $1s$ or $1p$ state is partially occupied at $n \neq 2$, samples must be metallic in the band picture. All of experimental results, however, show insulating properties, as mentioned above. According to the calculation [31], the unscreened Coulomb repulsion energy of two $1p$-electrons in the same cluster is estimated to be about 4 eV. This value is much larger than the calculated value of $1p$-band width $\sim$ 0.4 eV. Hence, the expectation of Mott-Hubbard insulating state is consistent with the experimental result.

4. Electron paramagnetic resonance and orbital degeneracy of potassium clusters in zeolite A

The g value of electrons in materials deviates from that of free electron value 2.00232, when the electrons have an SOI. The g value of free atoms with an orbital angular momentum is given by the Landé's g-formula, because of the rotational symmetry of free atoms. This value is much smaller than 2. In a solid, however, the crystal field quenches the orbital angular momentum even at a cubic symmetry. A small amount of orbital angular momentum appears by the mixing with higher excited states. If the electron in cluster contains a rotational part in degenerate quantum states, a finite orbital angular momentum recovers, which leads to an enhancement of the SOI at low temperatures. The g-value decreases in some degree from 2. At finite temperatures, cluster vibrations violate a rotational symmetry, and the SOI decreases. Therefore, the g value is quite sensitive to the symmetry and degeneracy of cluster.

We employed an X-band (9.7 GHz) electron spin resonance measurements for K clusters in zeolite A at paramagnetic temperatures. The K-loading density and the temperature dependences of g value reveal the SOI enhanced by the orbital degeneracy of $1p$ state. Possible structures of K clusters are also discussed. In Fig. 3, the g value of K clusters in zeolite A is plotted as a function of n [32]. The closed and open circles are the data measured at 10 and 300 K, respectively. The g value of bulk K metal is 1.9997 at liquid helium temperatures [33], as shown by horizontal dashed-and-dotted line in Fig. 3 for comparison. At $n < 2$, the g value is close to that of bulk K metal, and almost temperature independent. At $n > 2$, the g value suddenly decreases. The g value obviously decreases down to 1.996 at 10 K for 2

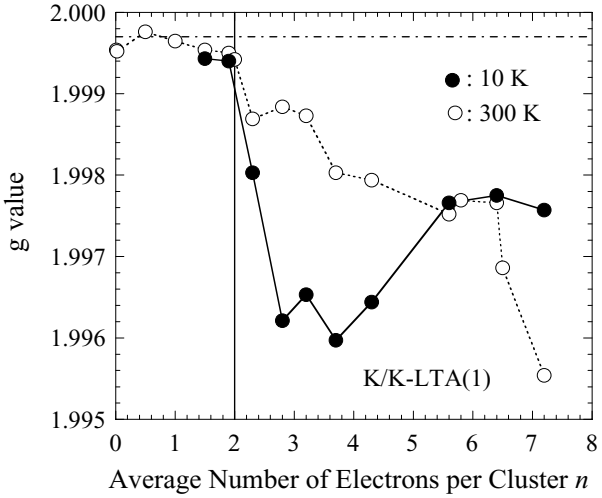

Fig. 3. The g value of K clusters in zeolite A as a function of the average number of electrons per cluster, n [32]. The g values are estimated from the electron paramagnetic resonance spectra measured by using X-band (9.7 GHz) microwave. Closed and open circles are for the values at 10 and 300 K, respectively. The horizontal dashed-and-dotted line indicates the g value of bulk K metal, 1.9997, at liquid helium temperatures [33].

$< n < 6$, and increases for $n > 6$. The g value at 300 K shows a remarkable decrease at $n = 7.2$. These results indicate that the SOI is large for $n > 2$. The temperature dependence for $n < 6$ is reverse to that for $n > 6$. The observed enhancement of the SOI in Fig. 3 can be explained by the orbital degeneracy of the $1p$ state of K cluster, as follows [32]. When $4s$ electrons of guest K atoms occupy the $1s$ state of K cluster for $n \leqslant 2$, the large SOI is not expected, because the $1s$ state has no orbital angular momentum. The SOI comes only from the contribution of the excited states. When n exceeds 2, $4s$ electrons of guest K atoms occupy the $1p$ state of K cluster. If the $1p$ orbital is degenerated and the orbital angular momentum is finite, the SOI is remarkably enhanced. If the degeneracy for $n > 6$ is not perfect, the SOI is reduced. At 300 K, molecular vibration may reduce the SOI for $n < 6$ and the g value shows intermediate value. Molecular vibration increases the degenerate component at 300 K for $n > 6$, then the SOI may increase at higher temperatures.

The α cage has the O_h symmetry, but the wave function of electrons is largely changed by the distribution of K cations. Hence, the triply degenerated state of $1p$ orbital can not be kept. Three cation sites are known in non-loaded zeolite A as shown in Fig. 4. The site I is near the 6-membered ring along the three-fold axis. There are eight equivalent positions in the unit cell. They are fully occupied by K cations as shown in Fig. 4(a) by the gray circles. The site II is in the plane near the center of the 8-membered ring, as shown by open (white) circles in Fig. 4(a). There are three equivalent positions of the site II, because the 8-membered ring is shared by adjacent α cage. They are fully occupied by K cations. Eleven K cations stay at sites I and II. One more cation exists in non-loaded zeolite A. The site III is beside the 4-membered ring inside the α cage, as shown by closed (black) circle in Fig. 4(a). There are twelve equivalent positions of site III in the α cage. One of these sites is occupied by the last K cation. This is called "twelfth cation". Then, totally twelve K cations are distributed in the α cage at the sites I, II and III in the non-loaded zeolite A. According to the structural analysis of K loaded K-form zeolite A [34,35], the extra K cations of the guest K atoms mainly occupy the empty position of site III. The fully occupied sites I and II can keep the O_h symmetry of α cage, but the cations at the site III may degrade the symmetry, because this site is not fully occupied even at the saturated sample at $n = 7.2$,

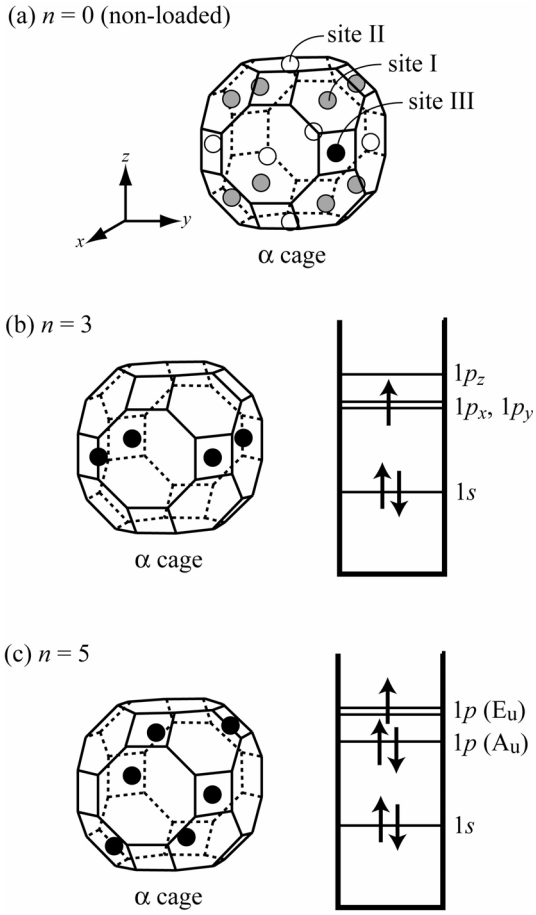

Fig. 4. (a) Schematic illustration of K^+ cation sites in the α cage of non-loaded zeolite A. (b) Possible cation arrangement in the α cage for K-loaded sample with $n = 3$ to realize the doubly degenerate $1p$ orbital occupied by an electron. The cation sites I and II are not shown here. The spin configuration in the electronic states of cluster is also shown in the right-hand-side of figure. (c) Same as (b) but for $n = 5$.

where 7 or 8 guest K atoms are loaded. This may quench the degeneracy of the $1p$ orbital. Hence, it is very hard to expect triply degenerate states of $1p$ orbital.

If we assume some cation configurations of the site III for the K-loaded samples, we can find doubly degenerated states as shown in Figs 4(b) and (c), where 3 and 5 guest K atoms are assumed at sites III, respectively. In Fig. 4(b), three guest cations and twelfth one are assumed at square form to have the C_4 symmetry, as shown in Fig. 4(b) (note that the cations in the sites I and II are neglected in this figure). Three s-electrons of guest K atoms occupy quantum states as shown in the right-hand-side of Fig. 4(b). In this case, $1p_x$ and $1p_y$ states are degenerated, and have the energy lower than $1p_z$ state because the cations have an attractive potential for electrons. Similarly, if we assume the five guest cations, as shown in Fig. 4(c), the C_3 symmetry can be realized. Of course, we can assume many other arrangements in the distribution of K cations different from that shown here. The x-ray structural analysis provides us only an average structure. There is no direct evidence of these local structures of K clusters at the present stage, but we can explain the orbital degeneracy of $1p$ state in K clusters in zeolite A, if we assume high symmetry structure as shown in Fig. 4.

5. Enhancement mechanism of spin-orbit interaction

Generally, the orbital degeneracy can be quenched by the Jahn-Teller effect at low temperature. However, if the spin-orbit interaction (SOI) energy is large enough to overcome the Jahn-Teller distortion, the lift of degeneracy can be suppressed. The quenching of the Jahn-Teller effect by the atomic spin-orbit coupling has been observed in the photoelectron spectra of small tin free-clusters [36] and also theoretically predicted in small lead clusters [37]. In the present alkali metal clusters, the atomic spin-orbit is absent, because of the closed shell structure of K cations and 4s-state of K atoms. From the microscopic point of view, the asymmetric potential induces 4p or higher atomic orbitals. The total SOI arises from the orbital angular momentum of 1p-state of cluster. This may be new type of phenomenon.

As discussed in the previous section, the doubly degenerate 1p-state is stabilized at low temperatures. With increasing temperature, the thermal vibration along the adiabatic potential may invalidate the effect of degeneracy, because symmetry of cluster dynamically deforms to lower symmetries. Then, the effective SOI decreases and the g value increases at higher temperature (the g value approaches 2). The observed temperature dependence of g value at $2 < n < 6$ can be explained by the above mechanism, indicating that the SOI is large enough to suppress the Jahn-Teller effect at low temperatures. On the other hand, for the saturated K-loading sample at $n = 7.2$, the orbital degeneracy is quenched due to the lower symmetry of cation arrangement. With increasing temperature, lower symmetry state can be dynamically hybridized with higher symmetry state. Then, the effective SOI increases and the g value decreases at higher temperatures (the g value deviates from 2).

For the quantitative estimation of the SOI of alkali-metal cluster, the jellium background model or the spherical-well potential one is quite insufficient and not applicable, because of the neglecting of local potential given by cation cores. Generally, the SOI H_{so} is proportional to the derivative of the static potential, namely $H_{so} \propto (\mathbf{l} \cdot \mathbf{s})/r \cdot dV\,(r)/dr$. In the jellium background model of cluster, the cation-core potential is averaged and the effective potential is quite smooth. This may give a negligibly small SOI. The actual potential of cluster, however, violently changes inside the cation-core. Hence, cations are expected to enhance the SOI.

In order to estimate the SOI including the effect of cation-cores, we need to improve wave functions of electrons, which are strongly modified inside the cation-cores, because the wave functions derived from the jellium background model are not orthogonalized to the cation-core wave functions. Smith calculated the spin-orbit splitting energy of the first optically excited state of the F centers in alkali halides by using the Schmidt orthogonalized wave function [38]. He succeeded to explain quantitatively the experimental values of spin-orbit splitting energy of the excited p-like state of F centers. We applied the Schmidt orthogonalized wave function to the alkali metal clusters in the zeolite cages and roughly estimated the SOI of the 1p state. In the case of K cluster, the wave functions of electrons are mainly constructed by 4s atomic orbital of K atoms, and an asymmetric potential induces the 4p-like atomic orbitals which contribute to the SOI of the cluster.

The Schmidt orthogonalized wave function [38] is given by

$$\phi_\mu = \frac{1}{\sqrt{(1 - \sum_\alpha S_{\mu\alpha}^2)}}(u_\mu - \sum_\alpha S_{\mu\alpha}\varphi_\alpha), \tag{1}$$

$$S_{\mu\alpha} = < u_\mu | \varphi_\alpha >, \tag{2}$$

where u_μ is the cluster wave function such as 1s-, 1p-, 1d-like orbitals, and φ_α the cation core wave function, such as 1s–3s or 2p_ν–3p_ν ($\nu = x,\ y,\ z$) orbitals in case of potassium, where the shell

configuration of K atom is given by $(1s)^2(2s)^2(2p)^6(3s)^2(3p)^6(4s)^1$. The function ϕ_μ is orthogonal to the occupied cation wave function:

$$< \phi_\mu | \varphi_\alpha >= 0. \tag{3}$$

Now, we assume that the cluster orbitals are $1p_x$, $1p_y$ and $1p_z$, and we denote u_μ as u_x, u_y and u_z, respectively. The expected value of the SOI for the orbital angular momentum of z-direction is calculated by the Schmidt orthogonalized wave functions of ϕ_x and ϕ_y. The SOI of cluster is measured by the energy difference, E_{SO}, between the states $^2\mathrm{P}_{3/2}$ and $^2\mathrm{P}_{1/2}$, where the respective rotational directions of orbital is parallel and antiparallel to that of spin:

$$E_{\mathrm{so}} = 2Re < \phi_x | H_{\mathrm{so}} | \phi_y > . \tag{4}$$

In usual calculation, a degeneracy of the $1p$-like state is assumed to be lifted, and non-degenerate orbitals are used for the calculation, because of the expectation of lower symmetry of cluster. In such case, the expected value of SOI is given by the perturbation term via the excited states. In the present model, however, the degeneracy of the orbital is kept, because the cluster in zeolite has a high symmetry. The expected value of Eq. (4) is given by the sum of three parts $< \phi_x | H_{so} | \phi_y >= \varepsilon_1 + \varepsilon_2 + \varepsilon_3$, where

$$\varepsilon_1 = \frac{1}{\sqrt{1 - \sum\limits_\alpha S_{x\alpha}^2}\sqrt{1 - \sum\limits_\alpha S_{y\alpha}^2}} < u_x | H_{so} | u_y >, \tag{5}$$

$$\varepsilon_2 = -\frac{1}{\sqrt{1 - \sum\limits_\alpha S_{x\alpha}^2}\sqrt{1 - \sum\limits_\alpha S_{y\alpha}^2}} \left[\sum_\alpha S_{x\alpha} < \varphi_\alpha | H_{\mathrm{so}} | u_y > + \sum_\beta S_{y\beta} < u_x | H_{so} | \varphi_\beta > \right], \tag{6}$$

$$\varepsilon_3 = \frac{1}{\sqrt{1 - \sum\limits_\alpha S_{x\alpha}^2}\sqrt{1 - \sum\limits_\alpha S_{y\alpha}^2}} \sum_{\alpha,\beta} S_{x\alpha} S_{y\beta} < \varphi_\alpha | H_{so} | \varphi_\beta > . \tag{7}$$

The term ε_1 is the cluster orbital term, ε_2 the cluster orbital vs. ion core term, and ε_3 the ion core term. If u is $1s$ cluster orbital, the expected value of SOI is zero, because the total angular momentum of cluster is zero. If u is $1p$ cluster orbital, the expected value becomes finite. The contributions of three terms are quite different. The values of ε_1 and ε_2 are expected to be very small, because the cluster potential given by the jellium background is quite smooth compared with the atomic potential. The derivative of this potential scarcely contributes to the SOI of cluster. The main contribution comes from the last term ε_3. This term can have a large value, only when both u_μ and φ_α have an orbital angular momentum. Main contribution comes from the term $\alpha \neq \beta$. Actually, $S_{x\alpha}S_{y\beta}$ has non-zero value, if α and β are ***np***$_x$ and ***np***$_y$ core orbitals of cations, respectively. This term is enhanced by the following two mechanisms in heavy alkali metals. One is the strong cation-size-dependence on $S_{xx}S_{yy}$. According to the rough estimation, $S_{xx}S_{yy}$ is proportional to the 5th power of cation size. The second reason is that the atomic SOI in the ***np*** states of ion core, $2 < \varphi_x | H_{so} | \varphi_y >$, is quite large. For example, the SOI energy of K^{2+}, namely $3p$ hole, is –268 meV. That of Na^{2+}, namely $2p$ hole, is –169 meV.

In order to make order estimation, we calculate the value of $S_{xx}S_{yy}$ under the some simplification of the wave functions. Here, we use $1p$ wave function given by the infinite spherical well potential as a trial function. Then, cluster wave functions u_x, for example, is given by

$$u_x = \sqrt{0.02482a}\frac{\sin(\beta r) - \beta r \cos(\beta r)}{r^3}x, \tag{8}$$

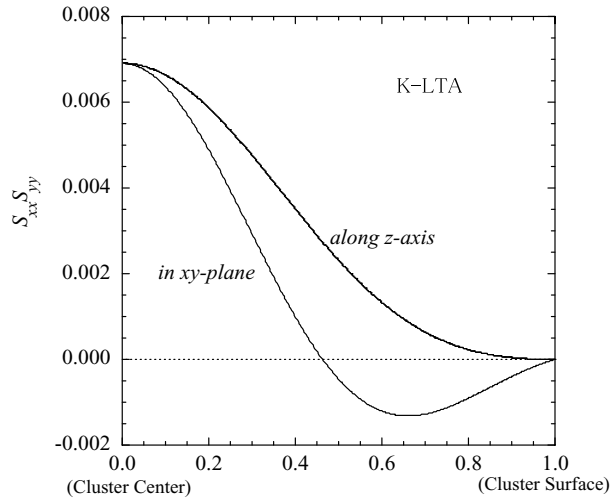

Fig. 5. A model calculation of spin-orbit interaction coefficient $S_{xx}S_{yy}$ for K cations located in the cluster with the radius of 5.5 Å. See the text for detail.

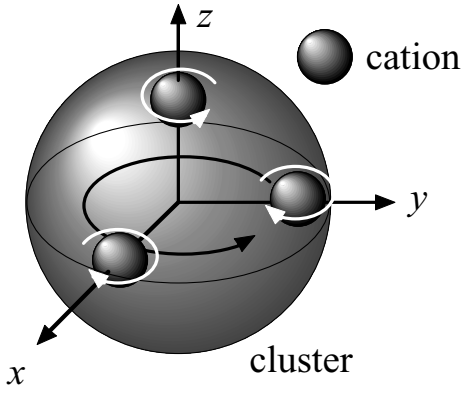

Fig. 6. Schematic illustration of $1p$ electron rotation and induced part surrounding cations.

where a is the radius of cluster, and β is given by$\beta a = 4.4934$. The true ion core wave function is complicated because of many electrons. In the present paper, we used $1p$ wave function with the size of cation, instead of the true core wave function. This assumption is bold, but tentatively enough to make the order estimation of the SOI.

The estimated value of $S_{xx}S_{yy}$ is given for K cation and cluster radii, 1.33 and 5.5 Å, respectively, in Fig. 5. The abscissa r/a means the cation position from the center of cluster. The r-dependence is calculated by the derivative of the $1p$ state. In the plot of $S_{xx}S_{yy}$, we choose two different axes for cation position; along z-axis and in the *xy*-plane. Schematic illustration of the rotation component of electrons surrounding cations is shown in Fig. 6. The rotation of $1p$ electron of cluster and that of induced p-like atomic wave function are indicated by black and white circles with arrows, respectively. The direction of rotation at cations in the *xy*-plane is opposite to that of $1p$ electron of cluster, as shown later.

The value in Fig. 5 indicates that the SOI strongly depends on the position and direction of cation. At

the center, $r = 0$, the value shows that the SOI is about 0.7% of cation core. Near the surface in the *xy*-plane, the SOI has a negative sign. At $r \sim 3.7$ Å ($r/a \approx 0.66$), for example, the value is –0.13%. In zeolite supported clusters, there are specific cation sites inside the α cage, and they are located at $r \approx$ 4 Å). Especially, it is noted that there is no cation at the center of cluster. The total value of SOI is given by the sum of the contribution of all cations and multiplied by the SOI of core electrons. The SOI contribution from a cation near z-axis poles is canceled by cations in *xy*-plane. If the number of cations near the *xy*-plane is larger than those near the z-axis poles, the sign of total SOI of $1p$ state in cluster is opposite to that in $4p$ state of K atom, where the energy of $^2\mathrm{P}_{3/2}$ state of K atom is 7.16 meV higher than that of $^2\mathrm{P}_{1/2}$ state. For example, in the structure shown in Fig. 4(b), the sign of total SOI of cluster is expected to be opposite to that in atomic SOI, similarly to that in F-center [38]. The number of cations included in the cationic cluster in *xy*-plane is eight including site II. The rough value of SOI is ten times of the SOI of cation in *xy*-plane. The total SOI amounts to about –1% of K atom core of $3p$ level at maximum. This value is about –3 meV. The negative value means that $^2\mathrm{P}_{3/2}$ state is lower than $^2\mathrm{P}_{1/2}$ state. This value may be over estimation, and the upper limit may be given. If we assume the structure shown in Fig. 4(c), the sign of SOI may be the same with that in the $4p$ state of K atom, and the value may be a few meV. For detailed discussion of the values, however, we need to improve the numerical calculation by using accurate wave function of clusters.

The SOI of cluster is also changed if the cluster contains many electrons. The SOI of cluster is formally given by the total orbital angular momentum *L* and total spin angular momentum *S* as $\lambda \mathbf{L} \cdot \mathbf{S}$, where λ is the SOI energy coefficient of cluster. The sign of λ usually changes depending on the total number of electrons. The SOI of hole has the opposite sign.

In an alkali-metal doped fullerene of Rb_3C_{60}, the ESR spectrum is much broader than that in K_3C_{60} [39]. The origin of the broadening is assigned to the enhancement of the SOI on Rb atoms. The conduction electrons mainly occupy the t_{1u} orbital of C_{60}. Formally, the SOI is possible for the degenerate t_{1u} orbital partly extended to Rb atoms. However, the main part of the wave function on the Rb atom is $5s$. Hence, we need a further explanation on the enhancement of SOI. According to the similar model presented here, the tail part of t_{1u} orbital induces $5p$-like orbital on Rb atom. The rotational motion of $5p$ electron on Rb atom is expected to enhance the SOI in the t_{1u} orbital of C_{60} in Rb_3C_{60}.

In nucleus, the shell structure of a single particle state of neutrons or protons has been well understood as the basic model of nuclear structure [40]. The single particle states, such as $1s$, $1p$, $1d$ states, are often calculated by the Woods-Saxon potential which is quite smooth as the function of distance from nuclear center. The SOI in nucleus plays an important role in the explanation of the magic number, such as 28, 50, 82, which are different from the regular magic number in the shell model, such as 20, 40, 70. The rather strong SOI in nucleus is explained by the short-range nucleonic two-body-interaction. This SOI has a large contribution near the nuclear surface, and is rewritten in the single particle potential form with the large SOI coefficient of the derivative term.

The SOI in alkali metal clusters has some analogy with that in nucleus. The single particle potential derived from the jellium model is quite insufficient for the explanation of the large SOI observed in experiments. The short-range two-body interaction between cluster electron and cation core electron plays an important role in the enhancement of the SOI, when the cluster electron has an orbital angular momentum. According to the Schmidt orthogonalized wave function technique, the derivative of the $1p$-like cluster electron wave function has a large contribution to the term ε_3, because of the derivative term of cluster wave function leads to a large expectation value of $S_{\mu\alpha}$ given in Eq. (2).

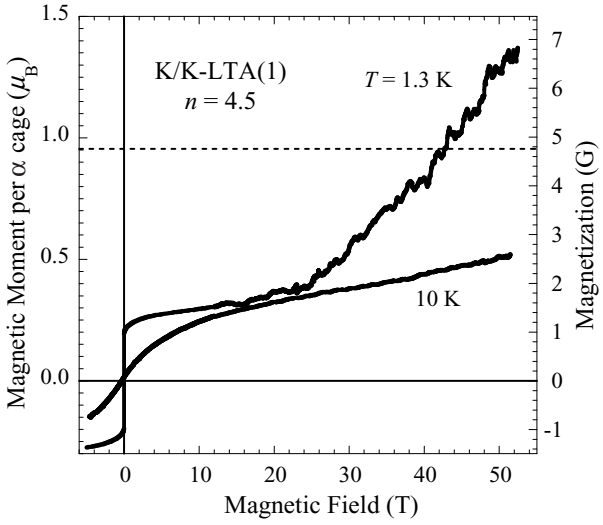

Fig. 7. Magnetization process up to 52 T for K clusters in zeolite A with $n = 4.5$ measured at 1.3 and 10 K. Horizontal dashed-line shows the maximum magnetization expected from the Curie constant (see text).

6. High magnetic field magnetization process and orbital degeneracy of potassium clusters in zeolite A

In this section, we show the magnetization process of K clusters in zeolite A. The detailed mechanism of this ferromagnetism will be discussed in the next section. An anomalously large magnetization was observed at high magnetic field at low temperatures in ferromagnetic samples [41]. Figure 7 shows the magnetization of K clusters in zeolite A with $n = 4.5$ measured at $T = 1.3$ and 10 K by using a pulsed magnet at KYOKUGEN, Osaka University [41]. The Curie temperature of present sample is ~ 6 K.

The magnetization at 1.3 K rises at very low fields due to the very soft ferromagnetism. The value of magnetization up to ~ 25 T increases slightly in proportion to the applied field H. The origin of the spontaneous magnetization of K clusters in zeolite A has been interpreted in terms of the spin-cant mechanism of antiferromagnetically ordered spins [42]. An H-linear increase at $H < 25$ T at $T = 1.3$ K in Fig. 7 can be well explained by the increase in the spin-canting angle [43]. At $H > 25$ T, however, the magnetization suddenly gains the increasing rate. The magnetization is still increasing at 52 T and amounts to 6.7 G for 1.3 K. This magnetization corresponds to the magnetic moment of ~ 1.3 μ_B per α cage (left hand side of the scale). On the other hand at 10 K, magnetization keeps a constant increasing rate up to 52 T. As shown in Fig. 8, the magnetic susceptibility, χ, of the present sample shows the Curie-Weiss law. The observed Curie constant $\sim 3.2 \times 10^{-4}$ K emu/cm^3 corresponds to $\sim$ 95% occupancy of the α cage with the magnetic moment of the spin quantum number $s = 1/2$ at $g = 2$. This value corresponds to 4.8 G (0.95 μ_B per α cage), as shown by the horizontal dashed-line in Fig. 7. Observed magnetization 6.7 G at 52 T for 1.3 K exceeds the value estimated from the Curie constant. It is noticed that the magnetization process in Fig. 7 cannot be explained by the frequently observed metamagnetic properties, such as a spin-flop behavior.

There have been several reports on the field-induced increase in magnetic moment of clusters, such as Cr-dimer complexes [44]. The stepwise increase in the magnetization is well understood as a spin-crossover between lower-spin and higher-spin states [44]. In these materials, the temperature dependence of magnetic susceptibility deviates from a Curie-Weiss law, because of a thermal distribution of multiple

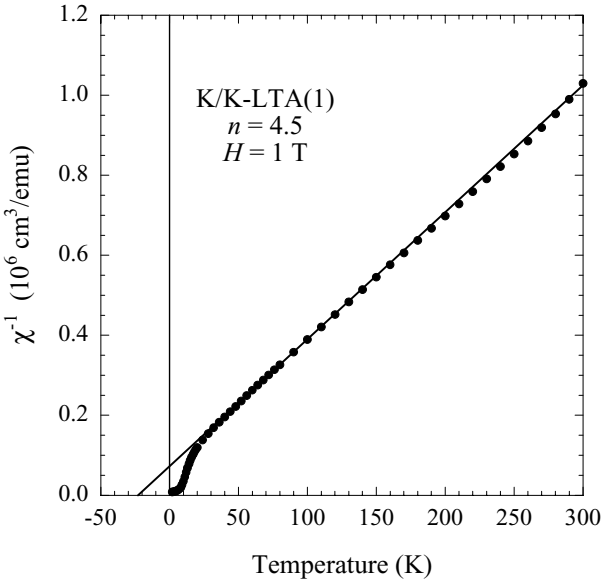

Fig. 8. Temperature dependence of the reciprocal of magnetic susceptibility for K clusters in zeolite A with $n = 4.5$. The Curie-Weiss law is clearly observed at higher temperatures as guided by solid line.

spin states. In K clusters in zeolite A, however, a Curie-Weiss law is clearly observed from $\sim$ 40 K up to the room temperature as seen in Fig. 8. Furthermore, the anomalous increase in the magnetization is observed only at low temperatures as seen in Fig. 7. Therefore, the mechanism of increase in the magnetization is different from an ordinary spin-crossover. Here, we propose a new mechanism based on a SOI in the degenerate $1p$ state of K cluster at low temperatures.

As mentioned in Section 4, the g value of the K clusters in zeolite A obviously decreases at low temperature for the samples with $2 < n < 6$. This result is interpreted in terms of a large SOI due to the degeneracy of the $1p$ state of cluster [32]. When the $1p$ state is triply degenerated in orbital, *LS* multiplet with an orbital angular momentum $L = 1$ and spin angular momentum $S = 1/2$ splits into two multiplets with the total angular momentum $J = 3/2$ and 1/2, because of the SOI. In a possible structure of K^+ cation arrangement inside the α cage (cluster), the doubly degenerate state may be possible as shown in Fig. 4(c), where five electrons are confined in a cluster. The non-degenerate $1p(A_u)$ state may have a lower energy than $1p(E_u)$ state due to the crystal field. Five s-electrons are confined in the cluster, where two for $1s$ state, two for $1p(A_u)$ state, and the last one for $1p(E_u)$ state. The $1p(E_u)$ state splits into two multiplets with $J_z = \pm 3/2$ and $\pm 1/2$, as shown in Fig. 9, where the first two electrons in $1s$ state are omitted. If the ground state of K cluster is the $J_z = \pm 1/2$ level of $1p(E_u)$ state at zero field, a crossover with the $J_z = \pm 3/2$ level of $1p(E_u)$ state will occur at a certain magnetic field, which is indicated by H_c in Fig. 9. Since $J_z = \pm 3/2$ state has a larger magnetic moment due to the contribution of the orbital magnetic moment, the magnetization may suddenly increase at a critical field, H_c. However, the z-axis of clusters is randomly oriented against the applied field in the powder sample. Hence, the increase in the magnetization results not in the stepwise but in the slope-wise change as observed in Fig. 7. If the ground state of K cluster is the $J_z = \pm 3/2$ or $1p_z$ state, an anomalous increase in magnetization is not expected.

If we assume the critical field, H_c, is 25 T from the magnetization curve in Fig. 7, the spin-orbit splitting energy can be estimated to be $\sim$ 1.5 meV from the Zeeman energy. This value is consistent with

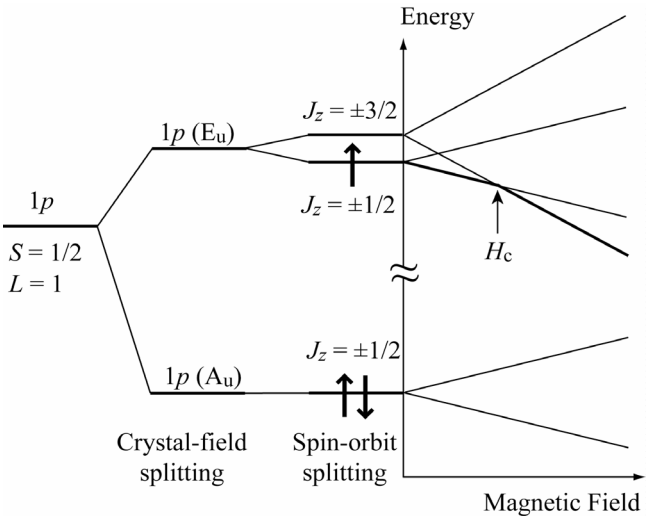

Fig. 9. Expected energy diagram of the degenerated $1p$ state of K cluster in α cage of zeolite A and its external-magnetic-field dependence. The $1p$ state has the orbital and spin angular momentums $L = 1$ and $S = 1/2$, respectively. The crystal field splitting is given as the doubly degenerated ground state in a structure model of Fig. 4(c). Five electrons including two in $1s$-state occupy the levels. Spin-orbit interaction makes a splitting of $1p$(E$_u$) state. If the ground state is the state $J_z = \pm 1/2$ at zero field, a crossover with the state $J_z = \pm 3/2$ will occur at the critical magnetic field H_C.

the order estimation given in Section 5. Therefore, the spin-orbit crossover mechanism for the sudden increase in the magnetization is consistent also from the quantitative point of view.

Sample with $n = 7.2$ shows a typical Curie law of paramagnetism without any intercluster interaction, although 75% of cages are occupied by the magnetic moment with spin 1/2 [30]. The non-degenerate orbitals of clusters may have an orthogonal orientation with each other. In this sample, the temperature dependence in g value is opposite to the samples at $2 < n < 6$ as shown in Fig. 3. The quench of orbital degeneracy can be explained by the lower symmetry of cation arrangement. The observed magnetization obeys Brillouin function without any anomalous increase in magnetization up to 50 T (the data are not shown here). This is because the orbital degeneracy is completely lifted at low temperatures, as discussed again in Section 7.

7. Ferromagnetism and orbital degeneracy of potassium clusters in zeolite A

K clusters in zeolite A is a quite novel ferromagnet, because the ferromagnetism is realized by the mutual interactions between s-electrons confined in the K clusters, and also magnetic element, such as $3d$ transition metal or $4f$ rare-earth metal, is not contained [10,26]. The magnetic interaction between clusters are realized by direct exchange interaction due to the overlap of wave functions of clusters through the window (8-membered ring) of the α cages [26]. According to the optical studies, this material is insulating at any value of K-loading density, n [29,30]. Hence, this material is assigned to the Mott-Hubbard type insulator as discussed in Section 3. Figure 10 shows the temperature dependence of magnetization for K clusters in zeolite A at $n = 4.5$ measured under the applied field of 100 Oe. The K-loading density of this sample is the same as that shown in Figs 7 and 8. With lowering temperature, the magnetization suddenly increases at ~ 7 K, and shows ferromagnetic value at lower temperatures. The Curie temperature 6 K is confirmed by the Arrott plot analysis of the temperature dependence of

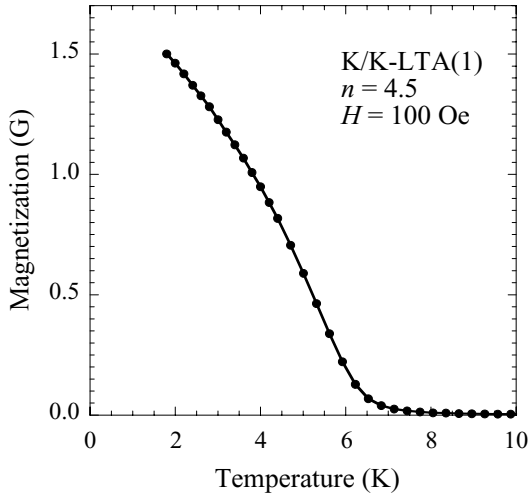

Fig. 10. Temperature dependence of magnetization of K clusters in zeolite A with $n = 4.5$ measured under the magnetic field of 100 Oe.

magnetization curve. At higher temperatures, the magnetic susceptibility obeys Curie-Weiss law with a negative Weiss temperature, T_W, as shown in Fig. 8 in the previous section. The negative value of T_W indicates the antiferromagnetic coupling between the magnetic moments of clusters. This result indicates that the spontaneous magnetization coexists with the antiferromagnetic coupling. Therefore, the ferromagnetic magnetization at low temperature is not ascribed to an ordinary ferromagnetism. The T_C and T_W show a strong n-dependence as summarized in Fig. 11 [30,45]. At $n \leqslant 2$, no magnetic ordering is observed above 1.8 K. The observed magnetic moment at low temperatures is very small compared to the number of loaded electrons. This result suggests that spin-singlet states are generated due to the dimerization of magnetic clusters at low temperatures [46]. At $n > 2$, the ferromagnetic property suddenly appears and T_C shows a finite value as seen in Fig. 11. The negative T_W develops, simultaneously. The T_C and the T_W show the maximum and minimum values of 7.5 K and –35 K, respectively, at around $n = 3.5$. Then, the absolute values of T_C and T_W decrease with increasing n, and continuously approach 0 K at the saturated K-loading density of $n = 7.2$.

The sudden appearance of ferromagnetism at $n > 2$ is clearly seen in the n-dependence of magnetization at 2 K, as shown in Fig. 12, where a weak external magnetic field of 5 Oe is applied [32]. The magnetization is shown in the logarithmic scale. It is emphasized that the magnetization shows a quick rise at $n = 2$ in several orders. The magnetization at $n \approx 4$, for example, is about four orders of magnitude larger than that at $n < 2$. It is clear that the spontaneous magnetization is observed only at $n > 2$. The maximum value of the magnetization is ~ 1.3 G at $n \sim 5$. This value corresponds to the magnetic moment of $\sim 0.26\ \mu_B$ per cluster. At $2 < n \leqslant 3$, the magnetization is more than one order of magnitude smaller than this value as seen in Fig. 12. On the other hand, the maximum saturation moment estimated from the Curie constant is nearly n-independent and is 0.8–1.0 μ_B per cluster at $n \gtrsim 3$ [42]. Hence, the value of spontaneous magnetization continuously changes with increasing n from a few percent to about 30 percent of the maximum saturation moment at $n > 2$.

According to the spherical well potential model of cluster shown in Fig. 2, the electrons of guest K atoms occupy the $1s$ state at $n \leqslant 2$. When n exceeds 2, the electrons start to occupy the $1p$ state. There is no doubt that the ferromagnetic phase boundary at $n = 2$ is in close relation to the electron occupation of the $1p$ state of K cluster. Therefore, it is concluded that the $1p$ state of K cluster is responsible for the

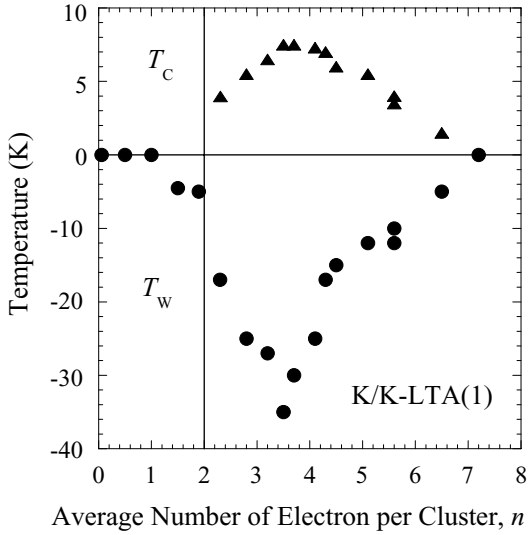

Fig. 11. The Curie temperature, T_C, and the Weiss temperature, T_W, of K clusters in zeolite A as a function of the average number of electron per cluster n. The T_C is estimated from the Arrott plot analysis of the magnetization curves. The T_W is estimated from the extrapolation of the Curie-Weiss law at higher temperatures.

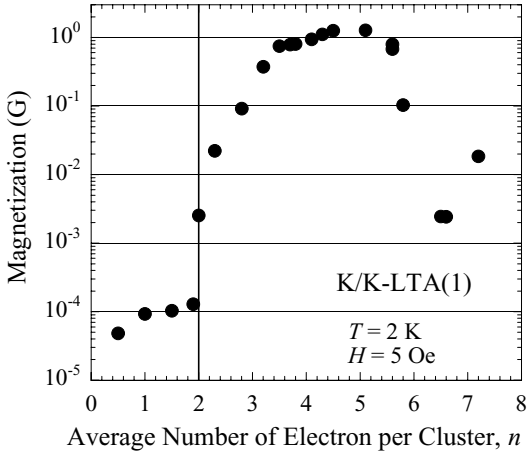

Fig. 12. Magnetization of K clusters in zeolite A measured at 2 K and 5 Oe as a function of the average number of electron per cluster n. The vertical axis is shown in the logarithmic scale.

spontaneous magnetization in K clusters in zeolite A. Moreover, as discussed in Section 4, the orbital degeneracy of the $1p$ state is stabilized at low temperature in the ferromagnetic samples with $2 < n < 6$. Hence, the orbital degeneracy of the $1p$ state may play an essential role in the spontaneous magnetization of ferromagnetism.

In order to explain the coexistence of the spontaneous magnetization and the antiferromagnetic coupling, two different mechanisms are possible in general. One is the ferrimagnetism, where the antiferromagnetic ordering of two (or more) magnetic sub-lattices with different magnetic moments generates the spontaneous magnetization. It is, however, not easy to explain the value of the spontaneous magnetization and its continuous increase with n [30,42]. Furthermore, a spin-flop behavior characteristic of

ferrimagnetism is not observed in the magnetization process up to 52 T as mentioned in Section 6 [41]. Therefore, the ferrimagnetism model is not applicable to the origin of spontaneous magnetization. The most plausible model is a weak ferromagnetism due to the canting of antiferromagnetically ordered magnetic moments. The spin-canting mechanism can explain a small spontaneous magnetization observed at $2 < n < 3$ and its continuous increase with n, because this can be understood by the change of the spin-canting angle. The magnetization curves at higher magnetic fields also can be explained by this model except for the crossover phenomena discussed in Section 6 [43].

In the muon spin relaxation (μSR) spectra, strong internal magnetic field of several hundred Oelsteds is observed below T_C [47,48]. The direction of the internal field is, however, found to be easily changed by a weak external field of ~ 10 Oe. This result seems anomalous, but the soft magnetization process of the spin-canted system can explain well the external-field sensitivity of the internal field [47,48]. Usually, the spin-canting interaction is caused by the Dzyaloshinsky-Moriya (DM) interaction [49,50]. The DM interaction (namely, the asymmetric exchange interaction) is given by the second-order perturbation through the SOI in the case of non-degenerated states. Hence, the DM interaction is usually much weaker than the isotropic exchange interaction. The DM interaction provides the spin canting with small angle to antiferromagnets, resulting in the small spontaneous magnetization. In ordinary spin-canted antiferromagnets, such as CoO_3 [51] or α-Fe_2O_3 [52], the value of the spontaneous magnetization is only in the order of one percent or less of the localized magnetic moment.

K clusters in zeolite A, however, exhibit much larger spontaneous magnetization, such as about 30% of the localized magnetic moment at the maximum. In order to explain such a huge value of magnetization, anomalously strong DM interaction should be assumed. According to the theory by Tachiki [53], the DM interaction is strongly enhanced by the orbital degeneracy up to the value comparable to the isotropic exchange interaction. As discussed in Section 4, the orbital degeneracy of the $1p$ state is realized at low temperature in the ferromagnetic samples with $2 < n < 6$. Therefore, the degeneracy may be the origin of the strong DM interaction resulting in the large spontaneous magnetization of K clusters in zeolite A. Usually, the appearance of the DM interaction is closely related to the symmetry of the magnetic ion sites, namely K cluster in the present sample. A superstructure has been observed in the x-ray diffraction experiment [54]. This is due to the periodic modulation of the number of K^+ cations in the α cages [34, 35]. The contrast of this modulation is found to increase with n [35]. The asymmetry of electronic potential between adjacent α cages may increase the DM interaction and decrease the isotropic exchange interaction. The superlattice structure may enhance the canting-angle, because the canting-angle is determined by the ratio of the DM interaction and the isotropic exchange interaction. A detailed analysis of the local structure, however, is required for the discussion of the integrated value of DM interaction in the three dimensionally arrayed $1p$ orbitals.

For the saturated K-loading sample at $n = 7.2$, the Curie's law is observed [30]. According to the analysis of the magnetization curve and the Curie constant, about 75% of α cages are occupied by the magnetic moment with the spin quantum number $s = 1/2$ [30]. It is strange that the interaction between magnetic moments of K clusters completely disappears, although the value of 75% exceeds sufficiently the percolation limit of a simple cubic lattice. In this sample, the orbital degeneracy is thought to be quenched as mentioned in Section 4. In a K cluster involving seven s-electrons, a hole state is generated in the $1p$ state, because of the occupation of five s-electrons in the $1p$ state. If the non-degenerate hole-orbitals of adjacent clusters are orthogonalized with each other, the exchange interaction between the holes in adjacent clusters may disappear. If the orthogonal-ordering of non-degenerate $1p$ orbitals is realized in the saturated K-loading sample, paramagnetism can be explained well. Further investigation is required to clarify the proposed orbital ordering at $n = 7.2$ by referring the structural analysis [34,35].

Recently, ferromagnetic properties are observed also in Rb clusters incorporated into zeolite A [23, 24]. The n-dependence of magnetic properties, however, is entirely different from that of K clusters. The ferromagnetism appears only at $n > 4$. The electron concentration of $n = 2$ is not the critical point in the appearance of ferromagnetism in Rb clusters, unlike K clusters. This result indicates that the orbital degeneracy of $1p$ state does not play an essential role for the ferromagnetism in Rb clusters. Therefore, the origin of the spontaneous magnetization in Rb clusters may be different from that in K clusters. A model of ferrimagnetism is proposed to explain the spontaneous magnetization of Rb clusters in zeolite A, where Rb clusters with non-equivalent magnetic moments are formed in the α and β cages, which are coupled antiferromagnetically [23,24].

Finally, the magnetically ordered states found in alkali-metal clusters in other zeolites are briefly mentioned here, and some comments are given from the viewpoint of the orbital degeneracy of cluster. Antiferromagnetic orderings have been found in Na [20] and K [55] clusters in sodalite (structural type code SOD) below the Néel temperatures of 48 and 72 K, respectively. In the SOD-type structure, the β cages are arrayed in a body centered cubic structure. In each β cage, an s-electron is trapped by four alkali cations, namely Na_4^{3+} or K_4^{3+} cluster. According to the spherical potential well model of cluster as shown in Fig. 2, one electron occupies the $1s$ state in these clusters. They are in the just-half filled condition to form a Mott-Hubbard insulator. The orbital degeneracy has no contribution to these materials. Several theoretical calculations have been also performed in Na and K clusters in sodalite [56–62].

The Néel's N-type ferrimagnetism is recently found in Na-K alloy clusters incorporated into low silica X zeolite (structural type code FAU) [27,63,64]. And also, very recently, new ferromagnetic state is found in K clusters in low silica X zeolite with high electron densities achieved by new technique of pressure doping [65,66]. In the FAU-type structure, two different cages, the β cages and the supercages of FAU, are arrayed in a diamond structure. The samples are thought to be metallic, and the stability of the ferrimagnetism or the ferromagnetism may be closely related to the itinerant electron ferromagnetism. The degeneracy is expected to contribute the stability of itinerant ferromagnetism. This point has attracted a deep interest in theoretical study, and sometimes discussed by using the degenerate Hubbard model. In the present cases of alkali-metal clusters, the degeneracy of $1p$- or $1d$-state is expected to enhance the stability of the itinerant electron ferromagnetism. This discussion is, however, rather speculative at the present stage. Further investigations are strongly required in order to clarify the origin of the ferrimagnetism and the ferromagnetism in the metallic states of these new systems.

8. Summary

We have shown novel electronic properties of alkali metal clusters stabilized in the nano-spaces of zeolite crystals. The properties are well explained by the electronic-shell model in K clusters arrayed periodically in zeolite A. The n- and temperature-dependences of g value indicate the orbital degeneracy of the $1p$ state of K clusters. Possible cation-arrangements of the clusters to realize the degenerated $1p$ orbital are also discussed. A rough estimation of SOI energy of the $1p$ state is given based on the Schmidt orthogonalized wave function. The anomalous increase in the magnetization at high magnetic field is explained by level crossing of *LS* multiplet terms in the degenerate $1p$ orbital. The origin of the ferromagnetic properties is interpreted in terms of spin-canted antiferromagnetism where the Dzyaloshinsky-Moriya interaction is expected to be strongly enhanced by the orbital degeneracy of the $1p$ state. The Mott-Hubbard type insulating state is realized by the large intra-cluster Coulomb energy compared to the inter-cluster electron-transfer energy. Magnetically ordered states of alkali-metal clusters in other zeolites are also discussed briefly from the viewpoint of the orbital degeneracy of cluster.

A wide variety of materials can be provided by the combination and control of host zeolites and guest metals. Novel electronic states of *supercrystal* (*crystal of superatoms*) realized in these materials open upon a rich field of material science.

Acknowledgements

We would like to thank Dr. S. Araki, Mr. T.C. Duan and Dr. Y. Ikemoto for fruitful discussions. YN would like to deeply thank Prof. H. Aoki and Dr. R. Arita for their continuous support and theoretical discussion. We are grateful to Prof. K. Kindo and Dr. A. Matsuo for their support in the high magnetic field experiments and fruitful discussions with them. We also acknowledge Prof. I. Watanabe and Dr. F.L. Pratt for their support in the μSR experiments and useful discussions. We also thank Mr. S. Tamiya for the chemical analysis. This work was partially supported by Grant-in-Aid for Creative Scientific Research (15GS0213), MEXT of Japan, also by the 21st Century COE Program named "Towards a new basic science: depth and synthesis".

References

[1] W.A. de Heer, *Rev Mod Phys* **65** (1993), 611.
[2] W.D. Knight, K. Clemenger, W.A. de Heer, W.A. Saunders, M.Y. Chou and M.L. Choen, *Phys Rev Lett* **52** (1984), 2141.
[3] M. Brack, *Rev Mod Phys* **65** (1993), 677.
[4] W. Ekardt, *Phys Rev B* **29** (1984), 1558.
[5] B. von Issendorff and O. Cheshnovsky, *Annu Rev Phys Chem* **56** (2005), 549.
[6] R. Kubo, *J Phys Soc Jpn* **17** (1962), 975.
[7] W.P. Halperin, *Rev Mod Phys* **58** (1993), 533.
[8] T. Welker and T.P. Martin, *J Chem Phys* **70** (1979), 5683.
[9] B. Mile, J.A. Howard, M. Histed, H. Morris and C.A. Hampson, *Faraday Discuss* **92** (1991), 129.
[10] Y. Nozue, T. Kodaira and T. Goto, *Phys Rev Lett* **68** (1992), 3789.
[11] H. van Bekkum, P.A. Jacobs, E.M. Flanigen and J.C. Jansen, Introduction to Zeolite Science and Practice (Studies in Surface Science and Catalysis, Vol. 137) Elsevier Science B. V. (2001).
[12] P.H. Kasai, *J Chem Phys* **43** (1965), 3322.
[13] J.A. Rabo, C.L. Angdll, P.H. Kasai and V. Schomaker, *Disc Faraday Soc* **41** (1966), 328.
[14] R.M. Barrer and J.F. Cole, *J Phys Chem Solids* **29** (1968), 1755.
[15] M.R. Harrison, P.P. Edwards, J. Klinowski and J.M. Thomas, *J Solid State Chem* **54** (1984), 330.
[16] P.P. Edwards, M.R. Harrison, J. Klinowski, S. Ramdas, J.M. Thomas, D.C. Johnson and C.J. Page, *J Chem Soc Chem Commun* **1984**, 982.
[17] F. Blatter, K.W. Blazey and A.M. Portis, *Phys Rev B* **44** (1991), 2800.
[18] T. Kodaira, Y. Nozue and T. Goto, *Mol Cryst Liq Cryst* **218** (1992), 55.
[19] A.R. Armstrong, P.A. Anderson, L.J. Woodall and P.P. Edwards, *J Phys Chem* **98** (1994), 9279.
[20] V.I. Srdanov, G.D. Stucky, E. Lippmaa and G. Engelhardt, *Phys Rev Lett* **80** (1998), 2449.
[21] Y. Ikemoto, T. Nakano and Y. Nozue, *Proceedings of the 12th International Zeolite Conference*, Baltimore, 1998, Vol. 3, Materials Research Society, 1999, p. 2103.
[22] Y. Ikemoto, T. Nakano, M. Kuno and Y. Nozue, *Physica B* **281&282** (2000), 691.
[23] T.C. Duan, T. Nakano and Y. Nozue, *J Magn Magn Mater* **310** (2007), 1013.
[24] T.C. Duan, T. Nakano and Y. Nozue, *e-J Surf Sci Nanotech* **5** (2007), 6.
[25] V.N. Bogomolov, *Usp Fiz Nauk* **124** (1978), 17 [*Sov Phys Usp* **21** (1978), 77].
[26] Y. Nozue, T. Kodaira, S. Ohwashi, T. Goto and O. Terasaki, *Phys Rev B* **48** (1993), 12253.
[27] T. Nakano, K. Goto, I. Watanabe, F.L. Pratt, Y. Ikemoto and Y. Nozue, *Physica B* **374–375** (2006), 21.
[28] T. Kodaira, Y. Nozue, S. Ohwashi, T. Goto and O. Terasaki, *Phys Rev B* **48** (1993), 12245.
[29] Y. Ikemoto, T. Nakano, Y. Nozue, O. Terasaki and S. Qiu? *Mater Sci Eng B* **48** (1997), 116.
[30] T. Nakano, Y. Ikemoto and Y. Nozue, *Eur Phys J D* **9** (1999), 505.
[31] R. Arita, T. Miyake, T. Kotani, M. Schilfgaarde, T. Oka, K. Kuroki, Y. Nozue and H. Aoki, *Phys Rev B* **69** (2004), 195106.

[32] T. Nakano, Y. Ikemoto and Y. Nozue, *J Phys Soc Jpn* **71**(Suppl) (2002), 199.
[33] W.M. Walsh, Jr., L.W. Rupp, Jr. and P.H. Schmidt, *Phys Rev* **142** (1966), 414.
[34] T. Ikeda, T. Kodaira, F. Izumi, T. Kamiyama and K. Ohshima, *Chem Phys Lett* **318** (2000), 93.
[35] T. Ikeda, T. Kodaira, F. Izumi, T. Ikeshoji and K. Oikawa, *J Phys Chem B* **108** (2004), 17709.
[36] V.D. Moravec, S.A. Klopcic and C.C. Jarrold, *J Chem Phys* **110** (1999), 5079.
[37] K. Balasubramanian and D. Majumdar, *J Chem Phys* **115** (2001), 8795.
[38] D.Y. Smith, *Phys Rev* **137** (1965), A574.
[39] K. Tanigaki, M. Kosaka, T. Manako, Y. Kubo, I. Hirosawa, K. Uchida and K. Prassides, *Chem Phys Lett* **240** (1995), 627.
[40] A. Bohr and B.R. Mottelson, *Nuclear Structure*, Vol. 1, *Single-Particle Motion*, 1st ed. by Benjamin, 1959, new ed. by World Scientific, 1998.
[41] T. Nakano, D. Kiniwa, A. Matsuo, K. Kindo and Y. Nozue, *J Magn Magn Mater* **310** (2007), e295.
[42] T. Nakano, Y. Ikemoto and Y. Nozue, *Physica B* **281**&**282** (2000), 688.
[43] T. Nakano, D. Kiniwa, Y. Ikemoto and Y. Nozue, *J Magn Magn Mater* **272–276** (2004), 114.
[44] T. Inoue, K. Sugiyama, T. Takeuchi, M. Nakahanda, S. Kaizaki and M. Date, *J Phys Soc Jpn* **61** (1992), 4566.
[45] T. Nakano, Y. Ikemoto and Y. Nozue, *J Magn Magn Mater* **226–230** (2001), 238.
[46] T. Nakano, Y. Ikemoto and Y. Nozue, *Mol Cryst Liq Cryst* **341** (2000), 461.
[47] T. Nakano, D. Kiniwa, F.L. Pratt, I. Watanabe, Y. Ikemoto and Y. Nozue, *Physica B* **326** (2003), 550.
[48] D. Kiniwa, T. Nakano, F.L. Pratt, I. Watanabe, Y. Ikemoto and Y. Nozue, *J Magn Magn Mater* **272–276** (2004), 117.
[49] I. Dzyaloshinsky, *J Phys Chem Solids* **4** (1958), 241.
[50] T. Moriya, *Phys Rev Lett* **4** (1960), 228; *Phys Rev* **120** (1960), 91.
[51] A.S. Borovik-Romanov and V.I. Ozhogin, *Soviet Phys J E T P* **12** (1961), 18.
[52] L. Néel, *Ann Physiq* **4** (1949), 249.
[53] M. Tachiki, *J Phys Soc Jpn* **25** (1968), 686.
[54] Y. Maniwa, H. Kira, F. Shimizu and Y. Murakami, *J Phys Soc Jpn* **68** (1999), 2902.
[55] L. Damjanovic, G.D. Stucky and V.I. Srdanov, *J Serb Chem Soc* **65** (2000), 311.
[56] A. Monnier, V. Srdanov, G. Stucky and H. Metiu, *J Chem Phys* **100** (1994), 6944.
[57] N.P. Blake, V.I. Srdanov, G.D. Stucky and H. Metiu, *J Phys Chem* **99** (1995), 2127.
[58] O.F. Sankey, A.A. Demkov and T. Lenosky, *Phys Rev B* **57** (1998), 15129.
[59] G.K.H. Madsen, C. Gatti, B.B. Iversen, Lj. Damjanovic. G.D. Stucky and V.I. Srdanov, *Phys Rev B* **59** (1999), 12359.
[60] R. Windiks and J. Sauer, *J Chem Phys* **113** (2000), 5466.
[61] G.K.H. Madsen, B.B. Iversen, P. Blaha and K. Schwarz, *Phys Rev B* **64** (2001), 195102.
[62] G.K.H. Madsen and P. Blaha, *Phys Rev B* **67** (2003), 85107.
[63] T. Nakano, K. Goto and Y. Nozue, to be submitted.
[64] M. Igarashi, T. Nakano, T. Shimizu, A. Goto, K. Hashi, K. Goto, K. Yamamichi and Y. Nozue, *J Magn Magn Mater* **310** (2007), e307.
[65] N.H. Nam, S. Araki, H. Shiraga, S. Kawasaki and Y. Nozue, *J Magn Magn Mater* **310** (2007), 1016.
[66] S. Araki, N.H. Nam, T. Ohtsu, C. Higashikawa, T. Nakano and Y. Nozue, to be submitted.